Tristetraprolin-mediated hexokinase 2 expression regulation contributes to glycolysis in cancer cells

Dong Jun Kim[a], Mai-Tram Vo[a], Seong Hee Choi[a], Ji-Heon Lee[b], So Yeon Jeong[a], Chung Hwan Hong[a], Jong Soo Kim[b], Unn Hwa Lee[a], Hyung-Min Chung[b], Byung Ju Lee[a], Wha Ja Cho[c,*], and Jeong Woo Park[a,*]

[a]Department of Biological Sciences and [c]Meta-Inflammation Research Center, University of Ulsan, Ulsan 680-749, Korea; [b]Department of Stem Cell Biology, School of Medicine, Konkuk University, Seoul 143-701, Korea

ABSTRACT Hexokinase 2 (HK2) catalyzes the first step of glycolysis and is up-regulated in cancer cells. The mechanism has not been fully elucidated. Tristetraprolin (TTP) is an AU-rich element (ARE)-binding protein that inhibits the expression of ARE-containing genes by enhancing mRNA degradation. TTP expression is down-regulated in cancer cells. We demonstrated that TTP is critical for down-regulation of HK2 expression in cancer cells. *HK2* mRNA contains an ARE within its 3′-UTR. TTP binds to *HK2* 3′-UTR and enhances degradation of *HK2* mRNA. TTP overexpression decreased HK2 expression and suppressed the glycolytic capacity of cancer cells, measured as glucose uptake and production of glucose-6-phosphate, pyruvate, and lactate. TTP overexpression reduced both the extracellular acidification rate (ECAR) and the oxygen consumption rate (OCR) of cancer cells. Ectopic expression of *HK2* in cancer cells attenuated the reduction in glycolytic capacity, ECAR, and OCR from TTP. Taken together, these findings suggest that TTP acts as a negative regulator of HK2 expression and glucose metabolism in cancer cells.

Monitoring Editor
A. Gregory Matera
University of North Carolina

Received: Oct 1, 2018
Revised: Dec 26, 2018
Accepted: Jan 8, 2019

INTRODUCTION

Cancer cell metabolism is characterized by enhanced uptake and utilization of glucose, a phenomenon known as the Warburg effect. While normal cells produce energy mainly through oxidation of pyruvate in mitochondria, cancer cells predominantly produce energy via enhanced glycolysis in the cytosol, regardless of whether they are under normoxic or hypoxic conditions (Warburg, 1956; Koppenol *et al.*, 2011). Cancer cells prefer to metabolize glucose by glycolysis to support proliferation and anabolic growth. They avoid oxidative phosphorylation even in the presence of sufficient amounts of oxygen, a property first observed by Otto Warburg (House *et al.*, 1956). The altered metabolism of cancer cells is connected with elevated lactate production and proton accumulation, which causes a drop in extracellular pH that promotes cancer metastasis (Bellone *et al.*, 2013). A correlation between glycolytic ATP production and tumor malignancy is reported (Simonnet *et al.*, 2002).

Hexokinase catalyzes the first committed step of the glycolytic pathway, in which glucose is phosphorylated to glucose-6-phosphate with concomitant dephosphorylation of ATP. Mammalian cells have four major HK isoforms: HK1, HK2, HK3, and HK4 (Wilson, 2003). Whereas HK1 is the most highly expressed hexokinase isoform and has no documented function in human cancer, HK2 is involved in cancer progression (Peschiaroli *et al.*, 2013). Up-regulation of HK2 is seen in multiple human cancers (Fang *et al.*, 2012), and HK2 is the most pivotal HK, with a direct function in the Warburg effect. HK2 is also essential for cancer growth, survival, and metastasis (Pedersen, 2007).

HK2 expression is reported to be regulated at epigenetic, transcriptional, and posttranscriptional levels. At the transcriptional level, HK2 expression is up-regulated by hypoxia-inducible factor-1α (HIF-1α) in cancer cells. The *HK2* promoter has a consensus motif

This article was published online ahead of print in MBoC in Press (http://www.molbiolcell.org/cgi/doi/10.1091/mbc.E18-09-0606) on January 16, 2019.

The authors declare no potential conflicts of interest.

*Address correspondence to: Wha Ja Cho (wjcho26@ulsan.ac.kr) or Jeong Woo Park (jwpark@ulsan.ac.kr).

Abbreviations used: ARE, AU-rich element; ECAR, extracellular acidification rate; G6P, glucose-6-phosphate; HK2, hexokinase 2; miRS, microRNA; OCR, oxygen consumption rates; TTP, tristetraprolin; 3′-UTRs, 3′-untranslated regions.

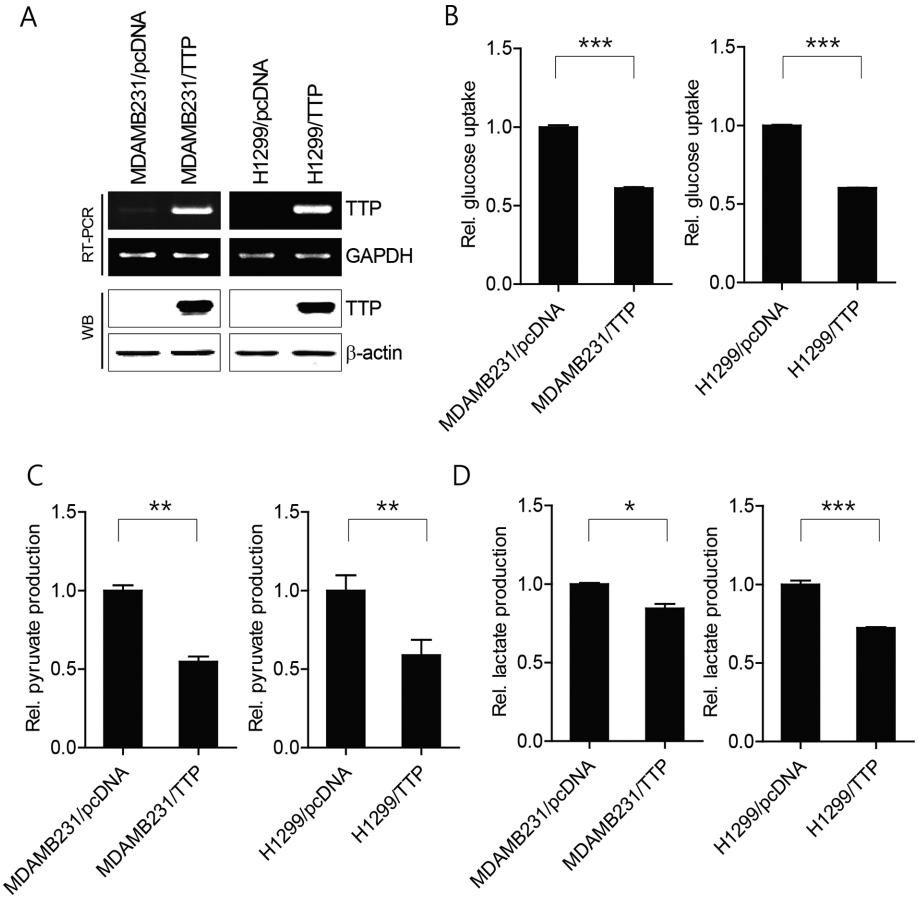

FIGURE 1: TTP overexpression decreases glycolytic capacity of cancer cells. MDAMB231 and H1299 cells were transiently transfected with 1 μg pcDNA6/V5-TTP (MDAMB231/TTP and H1299/TTP) or empty vector pcDNA6/V5 (MDAMB231/pcDNA and H1299/pcDNA) for 24 h. (A) TTP level was determined by semi-qRT-PCR (top) and Western blot (bottom). Cells were analyzed for (B) glucose uptake, (C) pyruvate production, and (D) lactate production. Data represent three experiments and are mean ± SD ($n = 3$; $*p < 0.05$; $**p < 0.01$; $***p < 0.001$).

for HIF-1 (Riddle *et al.*, 2000; Mathupala *et al.*, 2001) and expression is enhanced by hypoxia (Riddle *et al.*, 2000; Mathupala *et al.*, 2001; Gwak *et al.*, 2005; Kim *et al.*, 2007). Thus, *HK2* is considered to be a HIF-1α target gene (Semenza, 2003). In addition, c-Myc is reported to be involved in up-regulation of *HK2* in fibroblast growth factor–stimulated endothelial cells (Yu *et al.*, 2017). *HK2* expression might be epigenetically regulated, because DNA methylation of an *HK2* promoter CpG island suppresses *HK2* expression by inhibiting interaction between HIF-1α and a hypoxia response element in the *HK2* promoter (Lee *et al.*, 2016). At the posttranscriptional level, Roquin (An *et al.*, 2017) and several microRNAs (miRs) such as miR-199a-5p (Guo *et al.*, 2015), miR-4458 (Qin *et al.*, 2016), and miR-143 (Fang *et al.*, 2012; Peschiaroli *et al.*, 2013) are reported to target *HK2* mRNA and down-regulate *HK2* expression. Despite these findings, the regulation of *HK2* expression in cancer cells remains elusive.

Posttranscriptional regulation of gene expression can be mediated by AU-rich elements (AREs) located in the 3′-untranslated regions (3′-UTRs) of a variety of short-lived mRNAs such as those for cytokines and proto-oncogenes (Shaw and Kamen, 1986). The destabilizing function of AREs is regulated by ARE-binding proteins (Shyu and Wilkinson, 2000). One of the most well-characterized ARE-binding proteins is tristetraprolin (TTP), which promotes degradation of ARE-containing transcripts (Carballo *et al.*, 1998; Chen *et al.*, 2001; Lykke-Andersen and Wagner, 2005; Brooks and Blackshear, 2013). TTP inhibits cancer cell growth by inhibiting expression of cancer-related ARE-containing genes and enhancing degradation of proto-oncogene transcripts (Marderosian *et al.*, 2006; Young *et al.*, 2009; Lee *et al.*, 2010a,b). TTP inhibits the EMT through down-regulation of Twist1 and Snail1 (Yoon *et al.*, 2016). TTP expression is significantly decreased in various cancers (Brennan *et al.*, 2009), which may lead to abnormalities that contribute to cancer processes.

Here, we showed that TTP acted as a negative regulator of glycolysis by posttranscriptionally down-regulating *HK2* expression in cancer cells. Overexpression of TTP reduced glucose uptake, glycolysis, and growth of cancer cells. TTP did not affect the expression of HK1, but decreased HK2 expression by enhancing degradation of *HK2* mRNA. Exogenous expression of *HK2* restored glucose uptake, glycolysis, and growth of cancer cells. These novel findings suggested that TTP served as a negative regulator of HK2 in cancer cells. Considering the low levels of TTP in various cancers (Brennan *et al.*, 2009), these results suggested a mechanism for up-regulation of HK2 observed in human cancers.

RESULTS

TTP expression decreases the glycolytic capacity of cancer cells

We previously reported that TTP overexpression decreases mitochondrial potential and ATP production in cancer cells (Vo *et al.*, 2017). We investigated whether TTP expression affected the glycolytic capacity of cancer cells. MDAMB231 and H1299 cells were transfected with pcDNA6/V5-TTP (MDAMB231/TTP and H1299/TTP) or control pcDNA6/V5 vector (MDAMB231/pcDNA and H1299/pcDNA) to overexpress TTP. Cells were analyzed for glycolytic capacity. TTP overexpression in MDAMB231 or H1299 cells (Figure 1A) decreased glucose uptake (Figure 1B) and production of pyruvate (Figure 1C) and lactate (Figure 1D). We determined the effects of TTP inhibition on glycolytic capacity. MCF-7 and A549 cells were transfected with small interfering RNA (siRNA) against *TTP* (MCF-7/TTP-siRNA and A549/TTP-siRNA) or scramble control siRNA (MCF-7/scRNA and A549/scRNA) and analyzed for glucose uptake and pyruvate and lactate production. Inhibition of *TTP* by siRNA (Figure 2A) increased glucose uptake (Figure 2B) and production of pyruvate (Figure 2C) and lactate (Figure 2D). Taken together, these results indicated that TTP negatively regulated the glycolytic capacity of cancer cells.

TTP decreases expression of HK2 in cancer cells

TTP might inhibit the glycolytic capacity of cancer cells by down-regulating the expression of genes encoding enzymes in the glycolytic pathway. To test this hypothesis, we used reverse transcription PCR (RT-PCR) to determine the effect of overexpression or inhibition of TTP on expression of genes in the glycolytic pathway: *GLUT1*, *HK1*, *HK2*, *PKM2*, and *LDHA*. Among the five genes, TTP

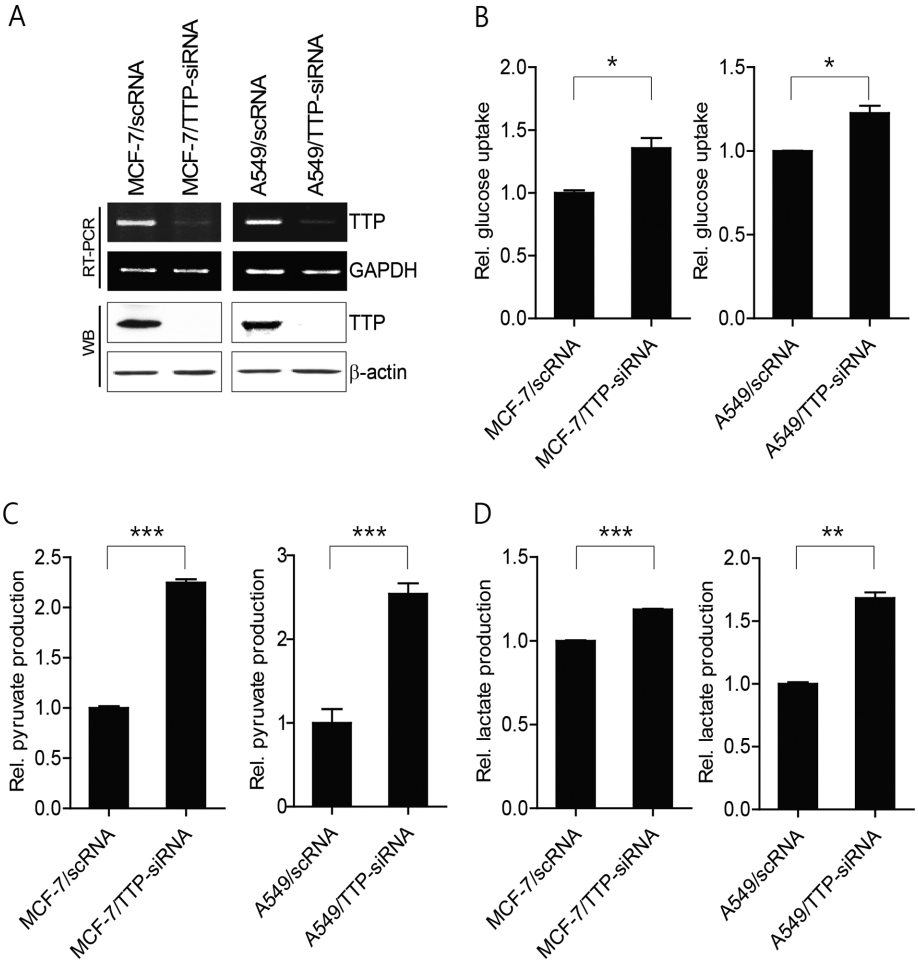

FIGURE 2: Inhibition of TTP by siRNA increases glycolytic capacity in cancer cells. MCF-7 and A549 cells were transfected with 60 pmol of TTP-specific siRNA (MCF-7/TTP-siRNA and A549/TTP-siRNA) or scRNA (MCF-7/scRNA and A549/scRNA) for 24 h. (A) TTP level was determined by semi-qRT-PCR (top) and Western blot (bottom). Cells were analyzed for (B) glucose uptake, (C) pyruvate production, and (D) lactate production. Data represent three experiments and are mean ± SD ($n = 3$; *$p < 0.05$; **$p < 0.01$; ***$p < 0.001$).

overexpression decreased only *HK2* in both MDAMB231 and H1299 cells (Figure 3A). The inhibition of *TTP* by siRNA increased expression of *HK2* and *LDHA* among the five genes tested in both MCF-7 and A549 cells (Figure 3B). We determined the effect of TTP overexpression on mRNA degradation of the five genes. TTP overexpression did not affect the mRNA stability of *GLUT1*, *HK1*, *PKM2*, and *LDHA* (Figure 3C), but enhanced degradation of *HK2* mRNA (Figure 3D) in both MDAMB23 and H1299 cells. These results indicated that TTP decreased HK2 expression by enhancing degradation of *HK2* mRNA. Previously, it has been reported that *HK2* mRNA stability is regulated by BAG3, Roquin, and Imp3 in cancer cells (An *et al.*, 2017). We thus tested whether TTP enhances *HK2* mRNA degradation by modulating the expression of these molecules. As shown in Figure 3E, overexpression or inhibition of TTP did not affect the expression levels of these molecules in either MDAMB231 or H1299 cells. These results suggest that these molecules are not involved in TTP-mediated degradation of *HK2* mRNA in cancer cells.

TTP decreases expression of luciferase mRNA containing the *HK2* 3′-UTR

Analysis of the 2429–base pair human *HK2* 3′-UTR revealed three pentameric AUUUA ARE motifs (Figure 4A). To determine whether down-regulation of *HK2* expression by TTP was mediated through the *HK2* mRNA 3′-UTR, we used a luciferase reporter gene linked to the full *HK2* 3′-UTR or a fragment containing all three AREs in the plasmid psiCHECK2. When MDAMB231 cells were transfected with plasmid to overexpress TTP, luciferase activity from the full (Figure 4B) or fragment (Figure 4C) *HK2* 3′-UTR was inhibited. To determine the AREs within *HK2* 3′-UTR that responded to TTP, we generated a luciferase reporter gene linked to oligonucleotides containing the first and second (oligo-ARE-1,2) or third AUUUA motif (oligo-ARE-3) in the plasmid psiCHECK2. Oligo-ARE-1,2 did not respond to TTP (Figure 4D), but luciferase activity from oligo-ARE-3W was inhibited by TTP overexpression (Figure 4E). To determine the importance of the third AUUUA motif, we prepared a luciferase reporter gene with mutant oligonucleotides (oligo-ARE-3M, containing AUUUA sequences substituted with AGCA). Oligo-ARE-3W responded to TTP but oligo-ARE-3M did not (Figure 4E). Taken together, these results demonstrated that the third AUUUA motif in the *HK2* 3′-UTR was involved in TTP inhibition in MDAMB231 cells.

TTP binds to the third ARE motif, ARE-3, in the *HK2* mRNA 3′-UTR

To determine whether TTP interacted with ARE-1,2 or ARE-3 of the *HK2* 3′-UTR, MDAMB231 cells were cotransfected with pcDNA6/V5-TTP and psiCHECK2-oligo-ARE-3W (oligo-ARE-3W), psiCHECK2-oligo-ARE-3M (oligo-ARE-3M), or psiCHECK2-oligo-ARE-1,2 (oligo-ARE-1,2). After immunoprecipitation with anti-V5 or control antibody (immunoglobulin G), the presence of TTP was determined by Western blots using anti-V5 (Figure 4F, bottom). Total RNA was extracted from immunoprecipitates, and the presence of luciferase mRNA was analyzed by RT-PCR using PCR primers specific to the luciferase gene. Amplified PCR product was observed in immunoprecipitates from cells cotransfected with oligo-ARE-3W and pcDNA6/V5-TTP (Figure 4F, top). No PCR products were detected in samples from cells cotransfected with pcDNA6/V5-TTP and oligo-ARE-3M or oligo-ARE-1,2 (Figure 4F, top). PCR product was also not detected in immunoprecipitates obtained using control antibody. We also determined the effect of TTP overexpression on mRNA degradation of the luciferase reporter genes linked to *HK2* AREs in MDAMB231 cells. TTP overexpression enhanced the mRNA degradation of reporter genes linked to a fragment containing all three AREs or ARE-3W of *HK2* but did not affect the mRNA stability of luciferase reporter genes linked to *HK2* ARE-3M or ARE-1,2 (Figure 4G). These results demonstrated that TTP interacted specifically with *HK2* ARE-3 and enhanced degradation of *HK2* ARE-3-containing mRNA.

TTP reduces hexokinase activity of cancer cells

HK2 is a key enzyme in the phosphorylation of glucose in glycolysis in cancer cells (Pedersen, 2007). We determined the effects of TTP

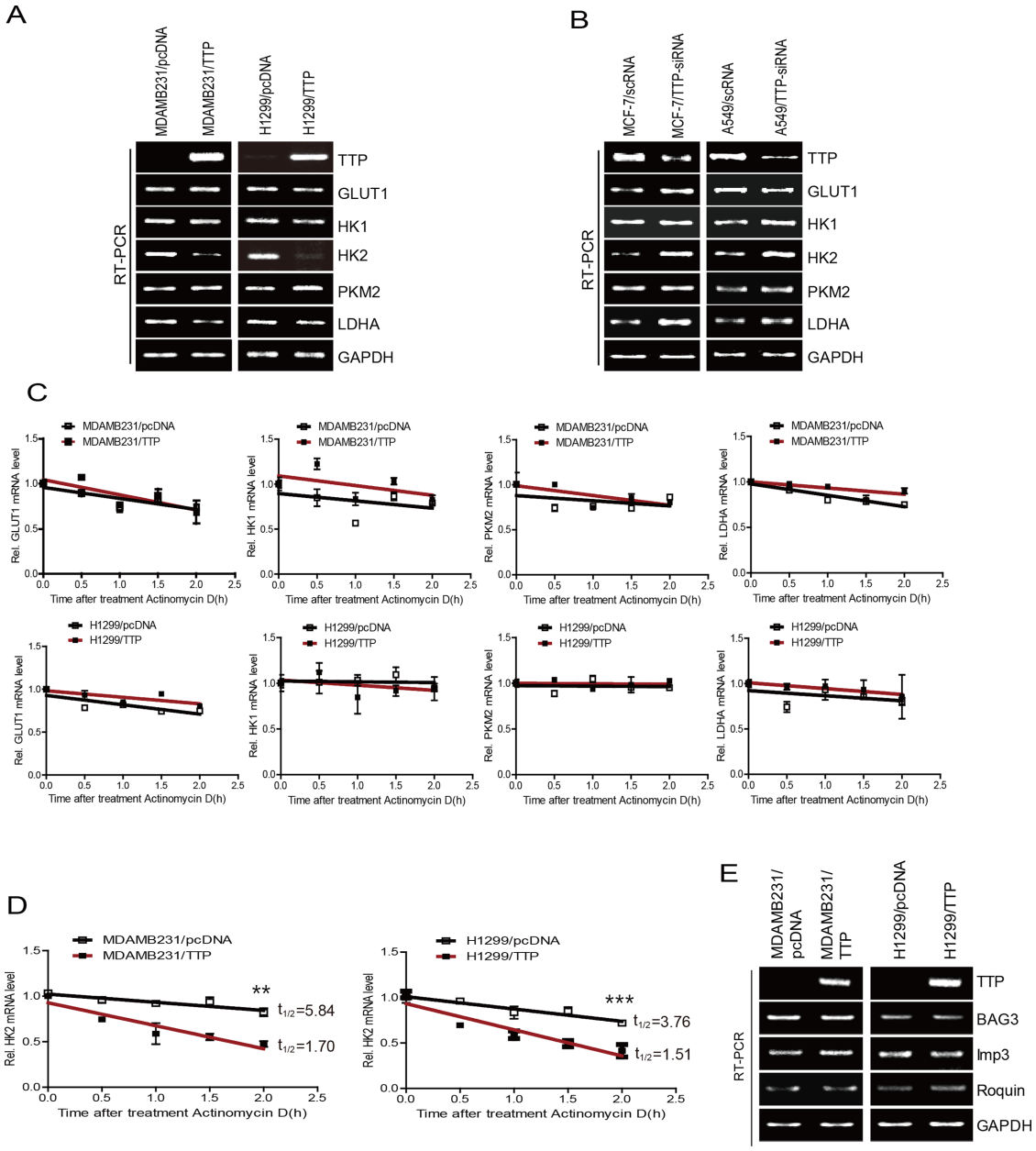

FIGURE 3: TTP enhances decay of *HK2* mRNA and reduces *HK2* expression in cancer cells. (A) TTP overexpression reduces *HK2* expression in cancer cells. MDAMB231 and H1299 cells were transiently transfected with pcDNA6/V5-TTP or pcDNA6/V5 for 24 h. Cells were analyzed by semi-qRT-PCR for *GLUT1*, *HK1*, *HK2*, *PKM2*, and *LDHA*. (B) Inhibition of TTP by siRNA increases *HK2* expression in cancer cells. MCF-7 and A549 cells were transiently transfected with TTP-specific siRNA or scRNA for 24 h. Cells were analyzed by semi-qRT-PCR for *GLUT1*, *HK1*, *HK2*, *PKM2*, and *LDHA*. (C, D) TTP destabilizes *HK2* mRNAs in cancer cells. MDAMB231 and H1299 cells were transiently transfected with pcDNA6/V5-TTP or pcDNA6/V5 for 24 h. Expression of (C) *GLUT1*, *HK1*, *PKM2*, *LDHA* and (D) *HK2* in cells was determined by qRT-PCR at indicated times after addition of 5 μg/ml actinomycin D. mRNA half-life was calculated from the nonlinear regression of the mRNA levels at the indicated times after addition of actinomycin D. Data are mean ± SD ($n = 3$; $^{**}p < 0.01$; $^{***}p < 0.001$). (E) TTP overexpression does not affect expression of *BAG3*, *Imp3*, and *Roquin* in cancer cells. MDAMB231 and H1299 cells were transiently transfected with pcDNA6/V5-TTP or pcDNA6/V5 for 24 h. Cells were analyzed by semi-qRT-PCR for *BAG3*, *Imp3*, and *Roquin*.

expression on hexokinase activity. Expression of HK2 correlated negatively with TTP in cancer cells: expression of HK2 in MDAMB231 and H1299 cells, which had low TTP, was higher than in MCF-7 and A549 cells, which had high TTP (Figure 5A). Overexpression of TTP in MDAMB231 and H1299 cells (Figure 5B) reduced hexokinase activity (Figure 5C). Inhibition of *TTP* by siRNA (TTP-siRNA; Figure 5D) enhanced hexokinase activity in MCF-7 and A549 cells (Figure 5E). These results suggested that TTP expression reduced hexokinase activity in cancer cells.

Ectopic expression of *HK2* attenuates reduction of glycolysis by TTP

On the basis of our results, we hypothesized that TTP controlled the glycolytic capacity of cancer cells by down-regulation of HK2. To

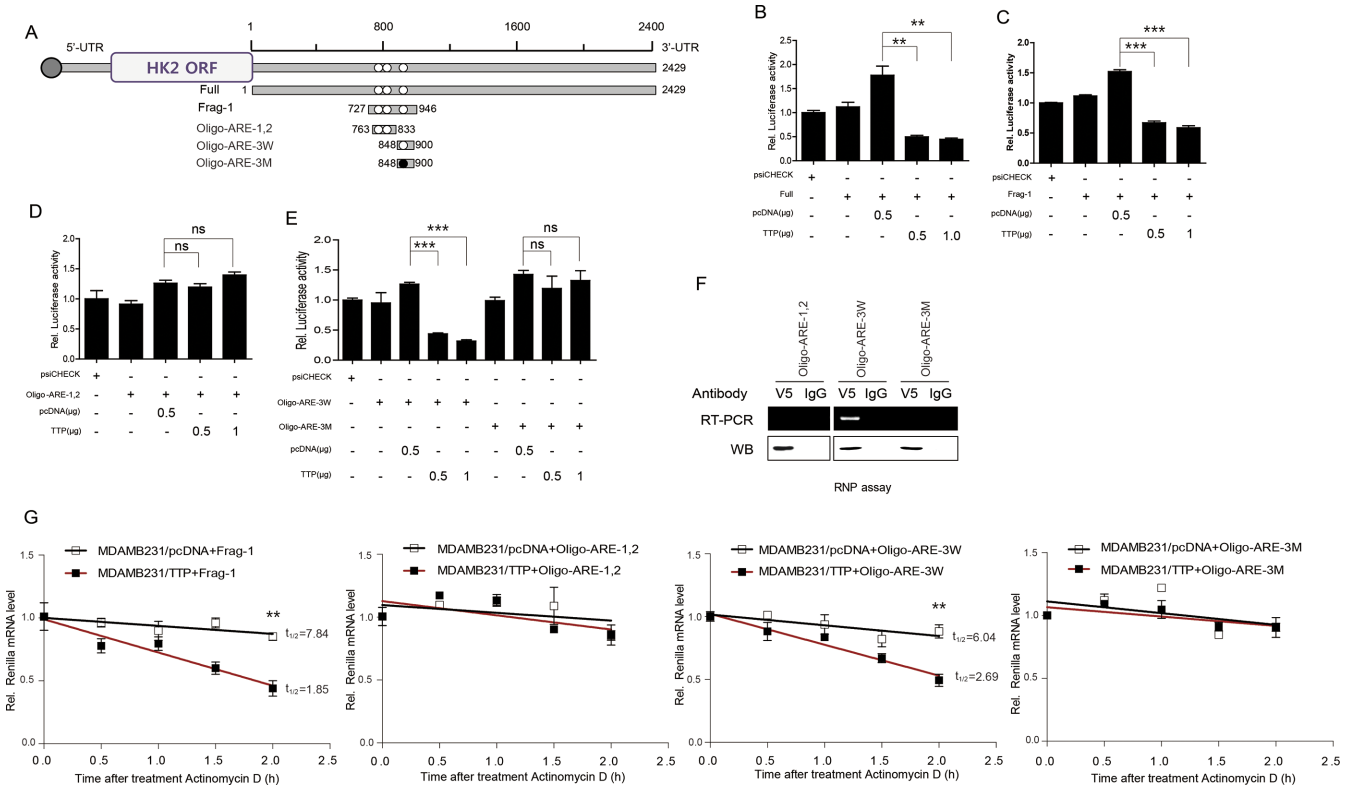

FIGURE 4: ARE-3 within the *HK2* mRNA 3′-UTR is essential for reduction by TTP. (A) Schematic representation of luciferase reporter constructs used in this study. (B–E) The third pentameric AUUUA motif within the *HK2* 3′-UTR is necessary for reduction by TTP. Full-length (Full), fragment (Frag), and oligonucleotides (Oligo) from the 2429–base pair *HK2* 3′-UTR were cloned downstream of the luciferase reporter gene in the psiCHECK2 luciferase expression vector. White circles, wild-type (W) pentameric motif AUUUA; black circle, mutated (M) motif AGCA. MDAMB231 cells were cotransfected with pcDNA6/V5-TTP and psiCHECK2 luciferase reporter constructs containing (B) full-length, (C) fragment, (D) oligo-ARE-1,2, and (E) oligo-ARE-3W or oligo-ARE-3M. After normalization, luciferase activity from the MDAMB231 cells transfected with the psiCHECK2 vector alone was set to 1.0. Data are mean ± SD ($n = 3$; $^{**}p < 0.01$; $^{***}p < 0.001$; ns, not significant). (F) Ribonucleoprotein immunoprecipitation assays. MDAMB231 cells were cotransfected with pcDNA6/V5-TTP and psiCHECK2 luciferase reporter constructs containing *HK2* oligo-ARE-1,2 or oligo-ARE-3W. The psiCHECK2 luciferase reporter construct containing mutant ARE-3, oligo-ARE-3M was the negative control. At 48 h after transfection, ribonucleoprotein complexes containing TTP were immunoprecipitated with protein G-agarose and anti-V5 or control antibody. Luciferase mRNA in immunoprecipitates was amplified by semi-qRT-PCR. TTP in immunoprecipitates was detected by Western blot with anti-V5. (G) TTP destabilizes luciferase reporter mRNA containing *HK2* oligo-ARE-3W but not *HK2* oligo-ARE-3M or *HK2* oligo-ARE-1,2. MDAMB231 cells were transiently cotransfected with pcDNA6/V5-TTP and psiCHECK2 luciferase reporter constructs containing fragment, oligo-ARE-1,2, oligo-ARE-3W, or oligo-ARE-3M for 24 h. Expression of luciferase reporter in cells was determined by qRT-PCR at indicated times after addition of 5 μg/ml actinomycin D. mRNA half-life was calculated from the nonlinear regression of the mRNA levels at the indicated times after addition of actinomycin D. Data are mean ± SD ($n = 3$; $^{**}p < 0.01$).

test this, we cotransfected MDAMB231 and H1299 cells with pcDNA6/V5-TTP and FLHKII-pGFPN3, which did not contain *HK2* 3′-UTR. At 24 h after transfection, cells were analyzed for glycolytic capacity. Expression of *HK2* (Figure 6A) significantly abrogated reduction by TTP of hexokinase activity (Figure 6B), glucose uptake (Figure 6C), and production of glucose-6-phosphate (G-6-P; Figure 6D), pyruvate (Figure 6E), and lactate (Figure 6F). These results indicated that TTP suppressed glycolytic capacity through down-regulation of HK2 in cancer cells.

TTP overexpression reduces extracellular acidification, oxygen consumption rates, ATP levels, and cell proliferation

Glycolysis is determined by measuring the extracellular acidification rate (ECAR) of media surrounding cells. Acidification is predominantly from excretion of lactic acid over time after conversion from pyruvate (Wu *et al.*, 2007). To evaluate the glycolytic phenotype, control and TTP-overexpressing cells were subjected to Seahorse Extracellular Flux Analysis to assess cellular bioenergetic activity. Results from glucose stress tests indicated that TTP overexpression significantly decreased ECAR associated with glycolysis, glycolytic capacity, and glycolytic reserve in MDAMB231 and H1299 cells (Figure 7, A and B). TTP overexpression also altered mitochondrial respiration using Seahorse Mito stress tests. Oxygen consumption rates (OCRs) associated with basal and maximal mitochondrial respiration were significantly down-regulated in TTP-overexpressing MDAMB231 and H1299 cells (Figure 7, C and D). Ectopic expression of *HK2* abrogated reduction of ECAR and OCR by TTP in both MDAMB231 and H1299 cells (Figure 7, A–D). We investigated ATP content and cell proliferation of TTP-overexpressing cells. Consistent with the decrease in ECAR and OCR, significant decreases in

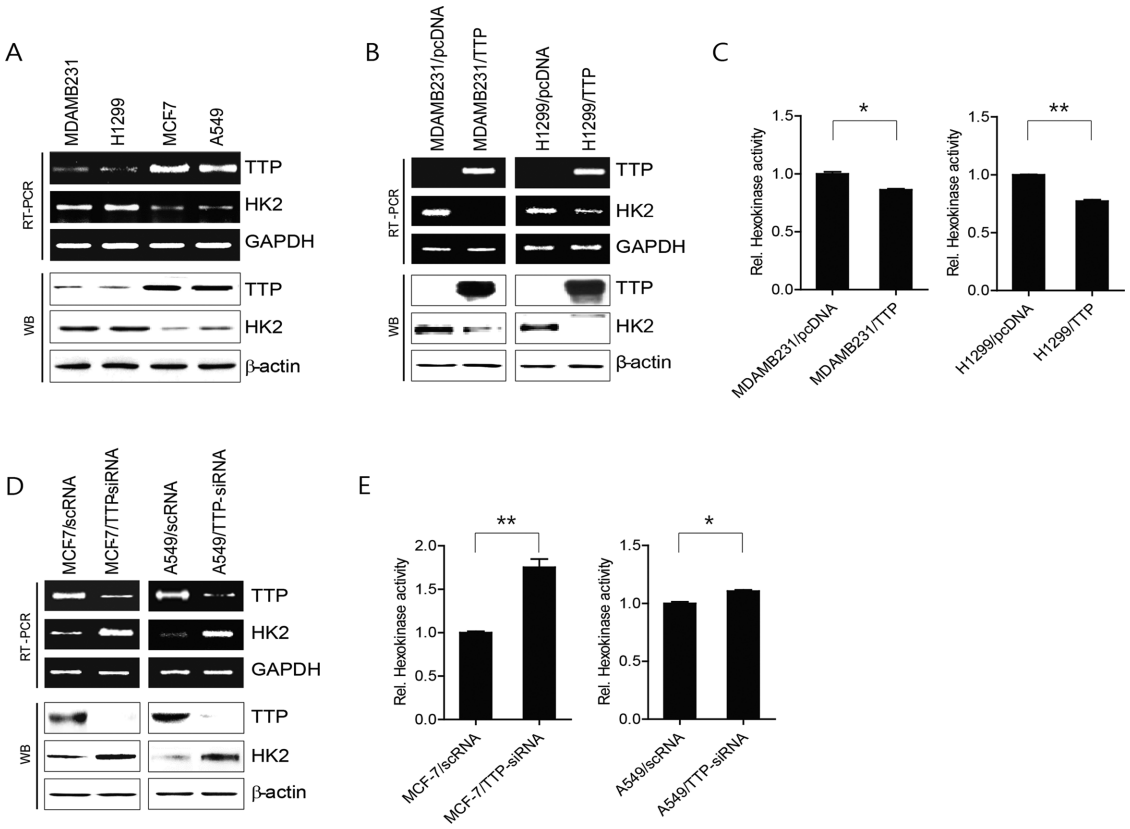

FIGURE 5: TTP reduces hexokinase activity in cancer cells. (A) Expression of HK2 negatively correlates with TTP in cancer cells. MDAMB231, MCF-7, H1299, and A549 cells were analyzed for TTP and HK2 by semi-qRT-PCR (top) and Western blot (bottom). (B, C) Overexpression of TTP decreases hexokinase activity in cancer cells. MDAMB231 and H1299 cells were transiently transfected with 1 μg pcDNA6/V5-TTP (MDAMB231/TTP) or pcDNA6/V5 (MDAMB231/pcDNA) for 24 h. Cells were analyzed for expression of TTP and HK2 by semi-qRT-PCR (top) and Western blot (bottom) (B) and for hexokinase activity (C). Data represent three experiments and are mean ± SD ($n = 3$; *$p < 0.05$; **$p < 0.01$). (D, E) Inhibition of *TTP* by siRNA increases hexokinase activity in cancer cells. MCF-7 and A549 cells were transfected with scRNA or TTP-specific siRNA (TTP-siRNA) for 24 h. Cells were analyzed for expression of TTP and HK2 by semi-qRT-PCR (top) and Western blot (bottom) (D) and for hexokinase activity (E). Data represent three experiments and are mean ± SD ($n = 3$; *$p < 0.05$; **$p < 0.01$).

ATP content and cell proliferation were observed in TTP-overexpressing MDAMB231 and H1299 cells (Figure 7, E and F). Ectopic expression of HK2 rescued the ATP content and cell proliferation in TTP-overexpressing MDAMB231 and H1299 cells (Figure 7, E and F). Taken together, these results demonstrated that overexpression of TTP reduced expression of HK2, followed by decreased glycolysis, mitochondrial respiration, ATP production, and cell proliferation in cancer cells.

DISCUSSION

HK2 is a key enzyme that catalyzes the rate-limiting first step of glycolysis and is highly up-regulated in multiple human tumors (Fang *et al.*, 2012). Here, we demonstrated that TTP acts as a key regulator of *HK2* expression and glycolysis in cancer cells. We provided evidence that *HK2* was a target of TTP: the *HK2* mRNA 3′-UTR contained an ARE, TTP decreased expression of a luciferase reporter gene linked to the *HK2* mRNA 3′-UTR, TTP bound to the *HK2* mRNA 3′-UTR, and overexpression of TTP enhanced degradation of *HK2* mRNA and decreased expression of HK2 in cancer cells. In addition, we found that TTP overexpression decreased glycolytic capacity. Ectopic expression of *HK2* abrogated reduction of the glycolytic capacity of cancer cells by TTP. Thus, our data indicated that TTP acted as a negative regulator of glycolysis through posttranscriptional down-regulation of *HK2* in cancer cells.

Four isoforms, HK1–HK4, are found in mammalian HKs (Wilson, 2003). Among these, HK2 is the predominantly overexpressed form in multiple human tumors (Fang *et al.*, 2012) and is essential for cancer growth, survival, and metastasis (Pedersen, 2007). We investigated the underlying mechanisms of increased expression of HK2 in tumors. Tumors use a multitude of genetic, epigenetic, transcriptional, and posttranslational strategies to enhance HK2 expression (Mathupala *et al.*, 2006). During tumorigenesis, the *HK2* gene is switched on by demethylation of the *HK2* gene promoter (Goel *et al.*, 2003). The *HK2* promoter contains well-defined cis-elements for transcription initiation (TATA and CAAT) and for activation by protein kinase-A and protein kinase-C pathways (Mathupala *et al.*, 1995; Rempel *et al.*, 1996; Lee and Pedersen, 2003). In addition, functional response elements for hypoxia via HIF-1 and p53 are located in the HK2 promoter (Mathupala *et al.*, 1997, 2001). Response elements in the proximal region of the *HK2* promoter required for its activity are either absent or poorly conserved in the promoters of *HK1*, *HK3*, and *HK4* (Lee and Pedersen, 2003). Roquin (An *et al.*, 2017) and several miRs such as miR-199a-5p (Guo *et al.*, 2015), miR-4458 (Qin *et al.*, 2016), and miR-143 (Fang *et al.*, 2012;

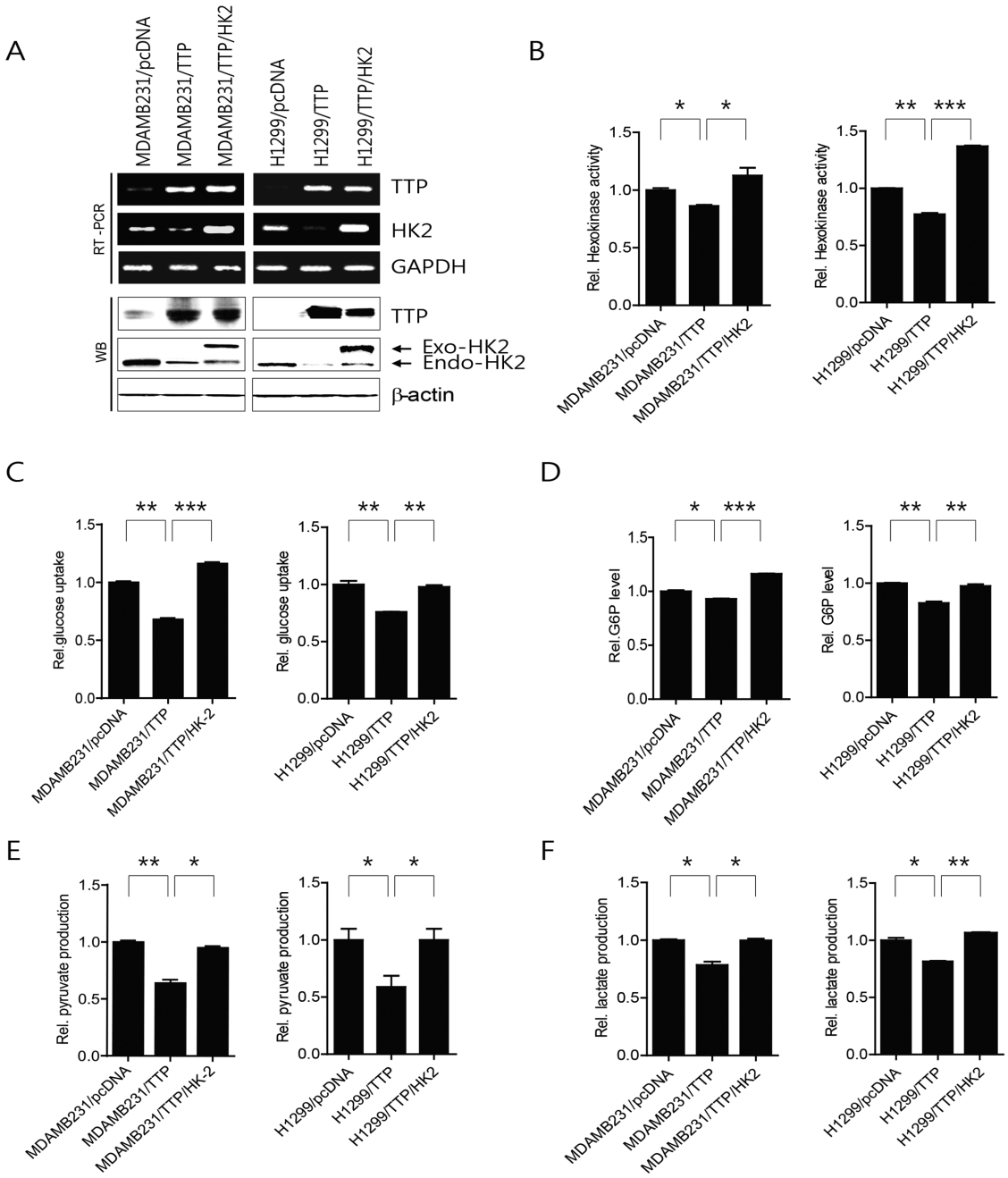

FIGURE 6: Overexpression of *HK2* attenuates reduction of glycolytic capacity of cancer cells by TTP. MDAMB231 and H1299 cells were transiently transfected with empty vector pcDNA6/V5 or pcDNA6/V5-TTP and FLHKII-pGFPN3 for 48 h. (A) TTP and HK2 levels were determined by RT-PCR (top) and Western blot (bottom). Cells were analyzed for (B) hexokinase activity, (C) glucose uptake, (D) G6P, (E) pyruvate production, and (F) lactate production. Data are mean ± SD ($n = 3$; $*p < 0.05$; $**p < 0.01$; $***p < 0.001$).

Peschiaroli *et al.*, 2013) are reported to target *HK2* mRNA and down-regulate HK2 expression. Although these findings help explain the selective expression of *HK2* in cancer cells, they are not sufficient to explain the enhanced expression of *HK2* in cancer cells, because these regulations may not occur only in tumor cells. In this study, we demonstrated that *HK2*, but not *HK1*, contains an ARE within its mRNA 3′-UTR. Thus, TTP reduced the expression of *HK2* but not *HK1* in human cancer cells. It has been reported that TTP expression is substantially decreased in 65% of human tumors derived from 19 different tissues and with particularly high frequency in tumors of the thyroid, lung, ovary, uterus, and breast (Brennan *et al.*, 2009). Considering that TTP acts as a negative regulator of HK2 expression in cancer cells, down-regulation of TTP in human tumors would critically contribute to up-regulation of HK2 and the Warburg effect in cancer cells.

HK2 binds to voltage-dependent anion channels (VDACs) on the outer mitochondrial membrane (Rose and Warms, 1967; Wilson, 1995) and preferentially accesses and uses mitochondrially generated ATP to phosphorylate glucose to glucose-6-phosphate (Arora and Pedersen, 1988). HK binding to VDACs is proposed to

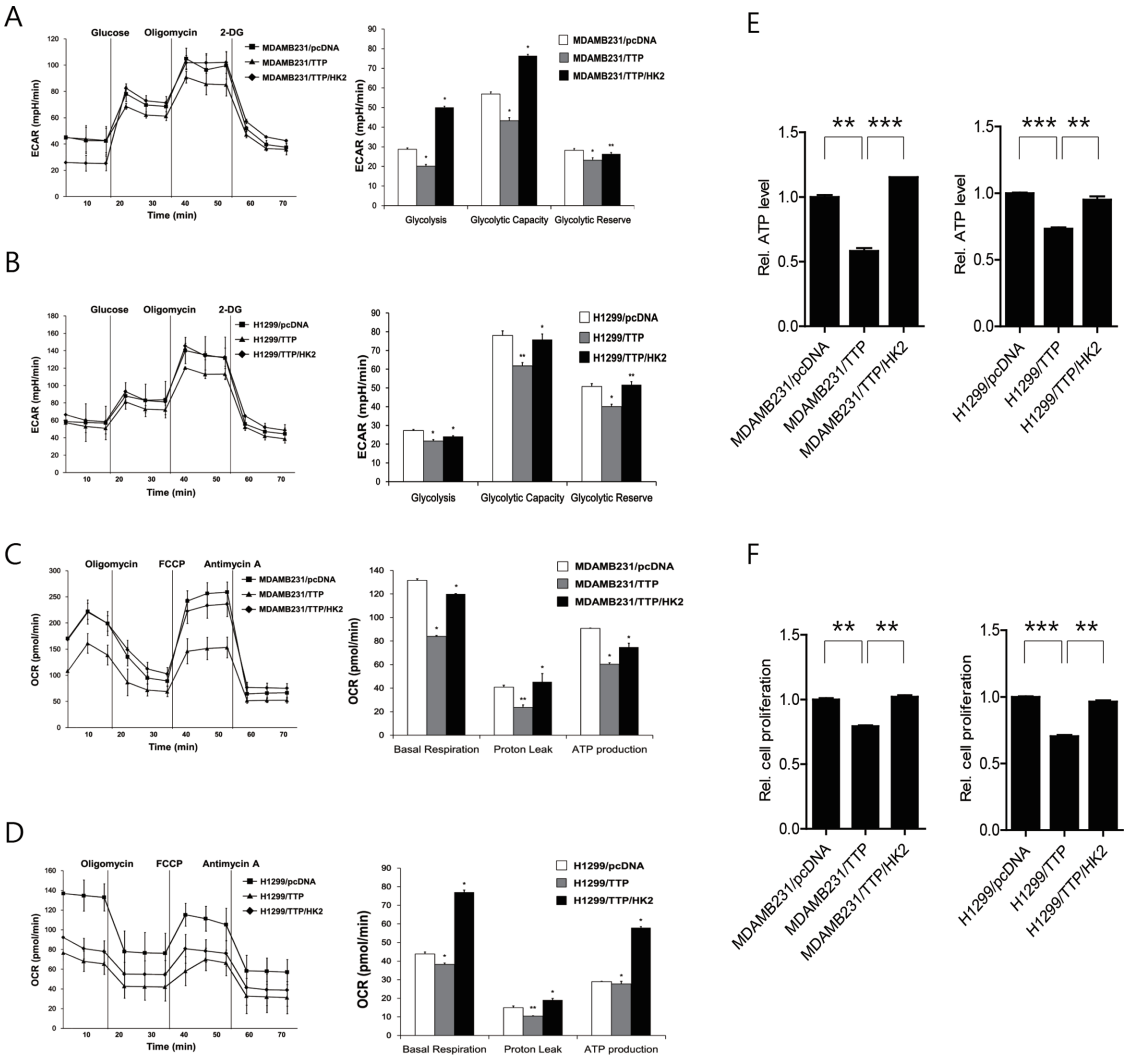

FIGURE 7: TTP overexpression decreases extracellular acidification rate (ECAR) and oxygen consumption rate (OCR) and ectopic expression of *HK2* attenuates TTP reduction of OCR and ECAR in cancer cells. MDAMB231 and H1299 cells were transiently transfected with empty vector pcDNA6/V5 or pcDNA6/V5-TTP and FLHKII-pGFPN3 for 48 h. (A–D) TTP overexpression decreases both ECAR and OCR in cancer cells. Mean ECAR in transiently transfected MDAMB231 cells (A) and H1299 cells (B) was measured before and after sequential addition of glucose (1 μM), oligomycin (1 μM), and 2-DG (1 μM). Each data point represents an ECAR measurement. Graphs show glycolysis, glycolytic capacity, and glycolytic reserve. Data are mean ± SD ($n = 3$; $*p < 0.05$; $**p < 0.01$). Mean OCR of transfected MDAMB231 cells (C) and H1299 cells (D) before and after addition of oligomycin (1 μM), FCCP (1 μM), or antimycin A (1 μM). Each data point represents an OCR measurement. Graphs are basal respiration, proton leak, and ATP production. Data are mean ± SD ($n = 3$; $*p < 0.05$; $**p < 0.01$). (E) TTP overexpression decreases cellular ATP levels in cancer cells. Cellular ATP from transfected MDAMB231 and H1299 cells, measured using the luminescent cell viability assays. Data are mean ± SD ($n = 3$; $*p < 0.05$; $**p < 0.01$; $***p < 0.001$). (F) TTP overexpression inhibits proliferation of cancer cells. Proliferation of transfected MDAMB231 and H1299 cells was assessed as absorbance at 490 nm using MTS cell proliferation assays. Graphs show relative cell proliferation. Data are mean ± SD ($n = 3$; $*p < 0.05$; $**p < 0.01$).

suppress mitochondrial function while stimulating glycolysis (Lemasters and Holmuhamedov, 2006). This proposal was in a report suggesting that inhibition of HK2 activity leads to a switch in bioenergetics from aerobic glycolysis to mitochondrial oxidative phosphorylation (Lu *et al.*, 2015). However, whether HK2 suppresses mitochondrial oxidative phosphorylation is controversial. Dissociation of HK2 from mitochondria is reported to inhibit glycolysis and mitochondrial respiration and deplete intracellular ATP levels (Woldetsadik *et al.*, 2017). Consistent with these findings, we found that down-regulation of *HK2* by TTP decreased both the oxygen consumption rate, mediated by mitochondria, and the glycolytic capacity of cancer cells. In addition, TTP overexpression decreased intracellular ATP in cancer cells. We previously reported that TTP induces mitochondrial dysfunction through down-regulation of α-synuclein (Vo *et al.*, 2017). Thus, we hypothesize that even though we did not determine the effect of TTP overexpression on α-synuclein level, TTP overexpression might inhibit mitochondrial oxidative phosphorylation through down-regulation of α-synuclein. We found that ectopic expression of HK2 rescued OCR and ECAR in TTP-overexpressed cancer cells, indicating that inhibition of mitochondrial oxidative phosphorylation and glycolysis by TTP was mediated by HK2 down-regulation. Collectively, our data suggested

that TTP reduced both mitochondrial oxidative phosphorylation and glycolysis through down-regulation of HK2 in cancer cells.

In this study, we found that the expression of *Glut1* and *LDHA* was induced by TTP inhibition. It is not likely that these genes are direct targets of TTP since TTP overexpression did not affect their mRNA stability. Glycolytic genes including *Glut1* and *LDHA* are induced by HIF-1α (Semenza *et al.*, 1994), whose expression and activity are modulated by mitochondrial dysfunction (Chandel *et al.*, 1998; Mansfield *et al.*, 2005). Considering that TTP can induce mitochondrial dysfunction (Vo *et al.*, 2017), it is possible that TTP may indirectly regulate the expression of *Glut1* and *LDHA* by inducing mitochondrial dysfunction.

In conclusion, our data suggested that TTP reduced both glycolysis and mitochondrial energy generation of human cancer cells through destabilization of *HK2* mRNA. We demonstrated that TTP enhanced degradation of *HK2* mRNA through binding to an AUUUA motif in the *HK2* mRNA 3′-UTR. *HK1* mRNA did not contain an AUUUA motif within its 3′-UTR. Thus, its expression was not regulated by TTP. Since TTP expression is inhibited in a variety of human cancer cells (Brennan *et al.*, 2009), HK2 up-regulation in cancer cells could be considered a consequence of low TTP levels in cancer. This study provided a molecular mechanism for the enhanced levels of *HK2* in cancer cells. TTP-mediated enhancing of *HK2* mRNA degradation expands our understanding of the regulation of *HK2* expression in cancer cells.

MATERIALS AND METHODS

Cell culture

The human cancer cell lines MDAMB231, H1299, MCF-7, and A549 were from the Korean Cell Line Bank (KCLB-Seoul, Korea). MDAMB231 cells were cultured in DMEM. H1299, MCF-7, and A549 cells were cultured in RPMI media. All cell lines were supplemented with 10% FBS (heat-inactivated fetal bovine serum; Welgene, Korea) and were maintained at 37°C under a humidified atmosphere of 5% CO_2.

Plasmids, small interfering RNAs, transfections, and dual-luciferase assays

The pcDNA6/V5-TTP construct was described previously (Lee *et al.*, 2010a,b). The FLHKII-pGFPN3 construct (Hossein Ardehali, Northwestern University) was from Addgene. MDAMB231 and H1299 cells were transfected with pcDNA6/V5-TTP or FLHKII-pGFPN3 using the TurboFect in vitro transfection reagent (R0531; Thermo Scientific).

siRNAs against human *TTP* (*TTP*-siRNA, sc-36760) and control siRNA (scRNA, sc-37007) were from Santa Cruz Biotechnology (Santa Cruz, CA). MCF-7 and A549 cells were transfected 24 h after plating using Lipofectamine RNAiMAX (13778-150; Invitrogen) and harvested at 48 h. Expression of TTP or HK2 mRNA and protein was analyzed by RT-PCR and Western blots.

A full-length version and a fragment of *HK2* 3′-UTR containing all three pentameric AUUUA motifs were amplified from MDAMB231 cDNA using the PCR primers HK2-3′-UTR Full-U, 5′-CCGCTCGAGAACCCCTGAAATCGGAAGGG-3′; HK2-3′-UTR-Full-D, 5′-ATAAGAATGCGGCCGCATTTTGGAAAATGTTAAAAT-3′; HK2-3′-UTR-Frag-U, 5′-CCGCTCGAGGTTTTACAAATTTTTCCTGC-3′; and HK2-3′-UTR-Frag-D, 5′-ATAAGAATGCGGCCGCCTGCCCTTTAACTACACTGA-3′. Underlined sequences are restriction enzyme sites. PCR products were inserted into the *XhoI*/*NotI* sites of the psiCHECK2 Renilla/Firefly dual-luciferase expression vector (Promega) to generate psiCHECK2-HK2 3′-UTR-Full and psiCHECK2-HK2 3′-UTR-Frag. Two oligonucleotides containing the first and the second pentameric AUUUA motifs (oligo-ARE-1,2) and the third pentameric AUUUA motif (oligo-ARE-3) of the *HK2* mRNA 3′-UTR were synthesized by ST Pharm (Korea; Table 1). Oligonucleotides were inserted into the *XhoI*/*NotI* sites of the psiCHECK2 expression vector. A mutant oligonucleotide with the AUUUA pentamer in the third AUUUA motif replaced with AGCA (oligo-ARE-3M) was also synthesized and ligated into the *XhoI*/*NotI* site of psiCHECK2. For luciferase assays, cells were cotransfected with indicated psiCHECK2-HK2 3′-UTR constructs and pcDNA6/V5-TTP using the TurboFect in vitro transfection reagent (R0531; Thermo Scientific). Transfected cells were lysed with lysis buffer and mixed with luciferase assay reagent (017757, Promega). Chemiluminescence signal was measured using a SpectraMax L microplate reader (Molecular Devices). Firefly luciferase was normalized to Renilla luciferase for each sample. Luciferase assays represent at least three independent experiments, each of three wells per transfection.

SDS–PAGE analysis and immunoblotting

Proteins were resolved by SDS–PAGE, transferred to nitrocellulose membranes (10600001; GE Healthcare), and probed with appropriate dilutions of anti-TTP (SAB4200505; Sigma), anti-HK2 (#2837; Cell Signaling), and anti–β-actin (A5441; Sigma). Immunoreactivity was detected using an ECL detection system (GE Healthcare). Films were exposed at multiple time points to ensure that images were not saturated. If required, band densities were analyzed with National Institutes of Health image software

Oligonucleotides	Sequences
Oligo-ARE-1,2	F: 5′-TCGAGTGGAATCACTGTATTTTCATTTTA**ATTTA**TATTTGAAATTTT**ATTTA**GTTCTTGATAGATCTGCTTCTTCGC-3′ R: 5′-GGCCGCGAAGAAGCAGATCTACTCAAGAAC**TAAAT**AAAATTTCAAATA**TAAAT**TAAAATGAAAATACAGTGATTCCAC-3′
Oligo-ARE-3W	F: 5′-TCGAGTGAATGGTCAGTTGTACGTAATTGT**ATTTA**TATGTTAATTTGTTATGTATATAGGC-3′ R: 5′-GGCCGCCTATATACATAACAAATTAACATA**TAAAT**ACATTACGTACAACTGACCATTCAC-3′
Oligo-ARE-3M	F: 5′-TCGAGTGAATGGTCAGTTGTACGTAATTGT**AGCA**TATGTTAATTTGTTATGTATATAGGC-3′ R: 5′-GGCCGCCTATATACATAACAAATTAACATA**TGCT**ACATTACGTACAACTGACCATTCAC-3′

Underlined sequences are restriction enzyme sites. Bold sequences are wild-type and mutant AU-rich elements.

TABLE 1: Oligonucleotides used to analyze *HK2* mRNA 3′-UTR.

and normalized by comparison with densities of internal control β-actin bands.

RNA kinetics, quantitative real-time PCR, and semiquantitative RT-PCR

For RNA kinetic analysis, we used actinomycin D (A9415; Sigma) and assessed *HK2* mRNA expression using quantitative real-time PCR (qRT-PCR). DNase I–treated total RNA (2 μg) was reverse-transcribed using oligo-dT (79237; Qiagen) and MMLV reverse transcriptase (3201; Beamsbio) according to the manufacturer's instructions. qRT-PCR was performed by monitoring increased fluorescence in real-time with the SYBR Green dye (MasterMix-R; Abm) using the StepOnePlus real-time PCR system (Applied Biosystems). Semiquantitative RT-PCR (semi-qRT-PCR) used Taq polymerase 2X premix (Solgent) and appropriate primers. PCR primer pairs were TTP, 5′-CGCTACAAGACTGAGCTAT-3′ and 5′-GAGGTAGAACTTGTGACAGA-3′; HK2, 5′-GGTGGACAGGATACGAGAAAAC-3′ and 5′-ACATCACATTTCGGAGCCAG-3′; GLUT1, 5′-CTTCACTGTCGTGTCGCTGT-3′ and 5′-TGAAGAGTTCAGCCACGATG-3′; HK1, 5′-TACTTCACGGAGCTGAAGGATG-3′ and 5′-CACCCGCAGAATTCGAAAGG-3′; PKM2, 5′-CTATCCTCTGGAGGCTGTGC-3′ and 5′-CCAGACTTGGTGAGGACGAT-3′; LDHA, 5′-GAGGTTCACAAGCAGGTGGT-3′ and 5′-CCCAAAATGCAAGGAACACT-3′; and GAPDH, 5′-ACATCAAGAAGGTGGTGAAG-3′ and 5′-CTGTTGCTGTAGCCAAATTC-3′. mRNA half-life was calculated by nonlinear regression of mRNA at 30-, 60-, 90-, and 120-min timepoints following addition of actinomycin D using GraphPad Prism 5.00 software based on a one-phase exponential decay model.

Ribonucleoprotein immunoprecipitation assays

To determine binding of TTP to *HK2* ARE, ribonucleoprotein immunoprecipitation (RNP) assays were conducted as described previously (Lee *et al.*, 2010b): MDAMB231 cells (1×10^7) were cotransfected with 10 μg pcDNA6/V5-TTP and psiCHECK2-HK2-oligo-ARE-3W or psiCHECK2-HK2-oligo-ARE-3M. At 24 h after transfection, cell suspensions were incubated in 1% formaldehyde for 20 min at room temperature. Reactions were stopped with 0.25 M glycine (pH 7.0), and cells were sonicated in modified radioimmune precipitation assay buffer containing protease inhibitors (Roche Applied Science). RNP complexes were immunoprecipitated using protein G-agarose beads preincubated with 1 μg anti-V5 Tag antibody (GWB-7DC53A, Genway Biotech) or 1 μg isotype control (Sigma). After cross-link reversion at 70°C for 45 min, RNA was isolated from immunoprecipitates and treated with DNase I (Qiagen). From the RNA, cDNA was synthesized, and the Renilla luciferase gene was amplified by PCR using *Taq* polymerase and Renilla luciferase-specific primers (Up, 5′-ACGTGCTGGACTCCTTCATC-3′; and Down, 5′-GACACTCTCAGCATGGACGA-3′). TTP proteins in immunoprecipitated samples were detected by Western blot using anti-V5 Tag.

Cell proliferation

Cells were transfected with a combination of pcDNA6/V5-TTP and FLHKII-pGFPN3 for 48 h. Cells were seeded in triplicate in 96-well culture plates at 5×10^3 cells/well and incubated for 24 h. Cells were measured with CellTiter 96 AQueous One Solution cell proliferation assays (Promega, 3580) according to the manufacturer's instructions, and absorbance at 490 nm was determined for each well using a Victor 1420 Multilabel Counter (EG&G Wallac, Turku, Finland).

ATP assays

Cellular ATP levels were measured using CellTiter-Glo luminescent cell viability assay kits (G7570; Promega) according to the manufacturer's instructions. MDAMB231 and H1299 cells were plated on 96-well white-walled plates with clear bottoms in 100 μl culture medium, and 100 μl CellTiter-Glo reagent was added to each well. Contents were mixed for 2 min on an orbital shaker to induce cellular lysis, followed by incubation at room temperature for 10 min to stabilize the signal. Luminescence was recorded immediately.

Glucose-6-phosphate assays

Glucose-6-phosphate (G6P) was measured using glucose-6-phosphate assay kits (MAK014; Sigma) according to the manufacturer's instructions: cells (1×10^6) were homogenized in two volumes of ice-cold PBS. After centrifugation at $13{,}000 \times g$ for 10 min to remove insoluble materials, 50 μl of supernatant was added to duplicate wells of 96-well plates. After addition of 50 μl reaction mix containing G6P Assay Buffer, G6P Enzyme Mix, and G6P Substrate Mix, absorbance at 450 nm was determined for each well using a Victor 1420 Multilabel Counter (EG&G Wallac, Turku, Finland).

Hexokinase assays

Hexokinase activity was measured using hexokinase colorimetric assay kits (MAK091, Sigma) according to the manufacturer's instructions: cells (1×10^6) were homogenized in 200 μl of ice-cold HK Assay Buffer. After centrifugation at $13{,}000 \times g$ for 10 min to remove insoluble materials, 50 μl supernatant was added to duplicate wells of 96-well plates. After addition of 50 μl reaction mix containing HK Assay Buffer, HK Enzyme mix, HK Developer, HK Coenzyme, and HK Substrate, absorbance at 450 nm was determined for each well using a Victor 1420 Multilabel Counter (EG&G Wallac, Turku, Finland).

Pyruvate assays

Pyruvate production was measured using pyruvate assay kits (MAK071; Sigma) according to the manufacturer's instructions: cells (1×10^6) were homogenized in four volumes Pyruvate Assay Buffer. After centrifugation at $13{,}000 \times g$ for 10 min to remove insoluble materials, 50 μl of supernatant was added to duplicate wells of 96-well plates. After addition of 50 μl reaction mix containing Pyruvate Assay Buffer, Pyruvate Probe Solution, and Pyruvate Enzyme Mix, absorbance at 570 nm was determined for each well using a Victor 1420 Multilabel Counter (EG&G Wallac, Turku, Finland).

Lactate assays

Lactate production was measured using lactate assay kits II (MAK065; Sigma) according to the manufacturer's instructions: cells (1×10^6) were homogenized in four volumes of Lactate Assay Buffer. After centrifugation at $13{,}000 \times g$ for 10 min to remove insoluble materials, 50 μl of supernatant was added to duplicate wells of 96-well plates. After addition of 50 μl reaction mix containing Lactate Assay Buffer, Lactate Enzyme Mix, and Lactate Substrate Mix, absorbance at 450 nm was determined for each well using a Victor 1420 Multilabel Counter (EG&G Wallac, Turku, Finland).

Glucose uptake assays

Glucose uptake was determined using Glucose Uptake-Glo assays (J1342; Promega) according to the manufacturer's instructions: cells (1.5×10^4) were seeded in wells of 96-well plates. After being washed with 100 μl PBS, cells were incubated with 50 μl 1 mM 2-deoxyglucose (2DG) per well for 10 min at room temperature. Cells were treated with 25 μl Stop Buffer, 25 μl Neutralization Buffer, and 100 μl 2-deoxyglucose-6-phosphate (2DG6P) Detection Reagent for 30 min at room temperature. Luminescence intensity was determined for each well using a Victor 1420 Multilabel Counter (EG&G Wallac, Turku, Finland).

Seahorse extracellular flux analysis

Glycolysis and mitochondrial stress tests were performed using an XF96 Extracellular Flux Analyzer (Seahorse Bioscience) according to the manufacturer's instructions. Cells were seeded at 1.5×10^4 cells per well in XF96 cell culture microplates and incubated for 24 h to ensure attachment. To measure oxygen consumption, cells were equilibrated for 1 h in unbuffered XF assay medium supplemented with 25 mM glucose, 1 mM sodium pyruvate, 2 mM glutamax, 1× nonessential amino acids, and 1% FBS in a non-CO_2 incubator. Mitochondrial processes were examined through sequential injections of oligomycin (1 μM), carbonyl cyanide 4-(trifluoromethoxy) phenylhydrazone (FCCP; 1 μM), and rotenone (1 μM)/antimycin A (1 μM). Indices of mitochondrial function were calculated as basal respiration rate (baseline OCR-rotenone/antimycin A OCR), ATP production (basal respiration rate-oligomycin OCR), and proton leak (oligomycin OCR-rotenone/antimycin A OCR). To measure glycolysis and glycolytic capacity, cells were cultured for 2 h in the absence of glucose. Three sequential injections of D-glucose (1 μM), oligomycin (1 μM), and 2-deoxyglucose (500 mM) provided ECAR associated with glycolysis, maximum glycolytic capacity, and nonglycolytic ECAR. Glycolysis was defined as ECAR following the addition of D-glucose and maximum glycolytic capacity was defined as ECAR following the addition of oligomycin. ECAR following treatment with 2-deoxyglucose is associated with nonglycolytic activity.

Statistical analysis

For statistical comparisons, p values were determined using Student's t test or one-way analysis of variance. A p value of <0.05 was considered significant.

ACKNOWLEDGMENTS

This study was supported by the National Research Foundation of Korea (NRF), funded by the Ministry of Education, Science and Technology (NRF-2014R1A6A1030318, NRF-2015R1D1A1A01059490, and NRF-2015M3A9C7030066).

REFERENCES

An MX, Li S, Yao HB, Li C, Wang JM, Sun J, Li XY, Meng XN, Wang HQ (2017). BAG3 directly stabilizes hexokinase 2 mRNA and promotes aerobic glycolysis in pancreatic cancer cells. J Cell Biol 216, 4091–4105.

Arora KK, Pedersen PL (1988). Functional significance of mitochondrial bound hexokinase in tumor cell metabolism. Evidence for preferential phosphorylation of glucose by intramitochondrially generated ATP. J Biol Chem 263, 17422–17428.

Bellone M, Calcinotto A, Filipazzi P, De Milito, A, Fais S, Rivoltini L (2013). The acidity of the tumor microenvironment is a mechanism of immune escape that can be overcome by proton pump inhibitors. Oncoimmunology 2, e22058.

Brennan SE, Kuwano Y, Alkharouf N, Blackshear PJ, Gorospe M, Wilson GM (2009). The mRNA-destabilizing protein tristetraprolin is suppressed in many cancers, altering tumorigenic phenotypes and patient prognosis. Cancer Res 69, 5168–5176.

Brooks SA, Blackshear PJ (2013). Tristetraprolin (TTP): interactions with mRNA and proteins, and current thoughts on mechanisms of action. Biochim Biophys Acta 1829, 666–790.

Carballo E, Lai WS, Blackshear PJ (1998). Feedback inhibition of macrophage tumor necrosis factor-alpha production by tristetraprolin. Science 281, 1001–1005.

Chandel NS, Maltepe E, Goldwasser E, Mathieu CE, Simon MC, Schumacker PT (1998). Mitochondrial reactive oxygen species trigger hypoxia-induced transcription. Proc Natl Acad Sci USA 95, 11715–11720.

Chen CY, Gherzi R, Ong SE, Chan EL, Raijmakers R, Pruijn GJ, Stoecklin G, Moroni C, Mann M, Karin M (2001). AU-binding proteins recruit the exosome to degrade ARE-containing mRNAs. Cell 107, 451–464.

Fang R, Xiao T, Fang Z, Sun Y, Li F, Gao Y, Feng Y, Li L, Wang Y, Liu X, *et al.* (2012). MicroRNA-143 (miR-143) regulates cancer glycolysis via targeting hexokinase 2 gene. J Biol Chem 287, 23227–23235.

Goel A, Mathupala SP, Pedersen PL (2003). Glucose metabolism in cancer. Evidence that demethylation events play a role in activating type II hexokinase gene expression. J Biol Chem 278, 15333–15340.

Guo W, Qiu Z, Wang Z, Wang Q, Tan N, Chen T, Chen Z, Huang S, Gu J, Li J, *et al.* (2015). MiR-199a-5p is negatively associated with malignancies and regulates glycolysis and lactate production by targeting hexokinase 2 in liver cancer. Hepatology 62, 1132–1144.

Gwak GY, Yoon JH, Kim KM, Lee HS, Chung JW, Gores GJ (2005). Hypoxia stimulates proliferation of human hepatoma cells through the induction of hexokinase II expression. J Hepatol 42, 358–364.

House SW, Warburg O, Burk D, Schade AL (1956). On respiratory impairment in cancer cells. Science 124, 267e272.

Kim JW, Gao P, Liu YC, Semenza GL, Dang CV (2007). Hypoxia-inducible factor 1 and dysregulated c-Myc cooperatively induce vascular endothelial growth factor and metabolic switches hexokinase 2 and pyruvate dehydrogenase kinase 1. Mol Cell Biol 27, 7381–7393.

Koppenol WH, Bounds PL, Dang CV (2011). Otto Warburg's contributions to current concepts of cancer metabolism. Nat Rev Cancer 11, 325–337.

Lee HG, Kim H, Son T, Jeong Y, Kim SU, Dong SM, Park YN, Lee JD, Lee JM, Park JH (2016). Regulation of HK2 expression through alterations in CpG methylation of the HK2 promoter during progression of hepatocellular carcinoma. Oncotarget 7, 41798–41810.

Lee HH, Son YJ, Lee WH, Park YW, Chae SW, Cho WJ, Kim YM, Choi HJ, Choi DH, Jung SW (2010a). Tristetraprolin regulates expression of VEGF and tumorigenesis in human colon cancer. Int J Cancer 126, 1817–1827.

Lee HH, Vo MT, Kim HJ, Lee UH, Kim CW, Kim HK, Ko MS, Lee WH, Cha SJ, Min YJ (2010b). Stability of the LATS2 tumor suppressor gene is regulated by tristetraprolin. J Biol Chem 285, 17329–17337.

Lee MG, Pedersen PL (2003). Glucose metabolism in cancer: importance of transcription factor–DNA interactions within a short segment of the proximal region of the type II hexokinase promoter. J Biol Chem 278, 41047–41058.

Lemasters JJ, Holmuhamedov E (2006). Voltage-dependent anion channel (VDAC) as mitochondrial governator—thinking outside the box. Biochim Biophys Acta 1762, 181–190.

Lu CL, Qin L, Liu HC, Candas D, Fan M, Li JJ (2015). Tumor cells switch to mitochondrial oxidative phosphorylation under radiation via mTOR-mediated hexokinase II inhibition—a Warburg-reversing effect. PLoS One 10, e0121046.

Lykke-Andersen J, Wagner E (2005). Recruitment and activation of mRNA decay enzymes by two ARE-mediated decay activation domains in the proteins TTP and BRF-1. Genes Dev 19, 351–361.

Mansfield KD, Guzy RD, Pan Y, Young RM, Cash TP, Schumacker PT, Simon MC (2005). Mitochondrial dysfunction resulting from loss of cytochrome c impairs cellular oxygen sensing and hypoxic HIF-alpha activation. Cell Metab 1, 393–399.

Marderosian M, Sharma A, Funk AP, Vartanian R, Masri J, Jo OD, Gera JF (2006). Tristetraprolin regulates Cyclin D1 and c-Myc mRNA stability in response to rapamycin in an Akt-dependent manner via p38 MAPK signaling. Oncogene 25, 6277–6290.

Mathupala SP, Heese C, Pedersen PL (1997). Glucose catabolism in cancer cells. The type II hexokinase promoter contains functionally active response elements for the tumor suppressor p53. J Biol Chem 272, 22776–22780.

Mathupala SP, Ko YH, Pedersen PL (2006). Hexokinase II: cancer's double-edged sword acting as both facilitator and gatekeeper of malignancy when bound to mitochondria. Oncogene 25, 4777–4786.

Mathupala SP, Rempel A, Pedersen PL (1995). Glucose catabolism in cancer cells. Isolation, sequence, and activity of the promoter for type II hexokinase. J Biol Chem 270, 16918–16925.

Mathupala SP, Rempel A, Pedersen PL (2001). Glucose catabolism in cancer cells: identification and characterization of a marked activation response of the type II hexokinase gene to hypoxic conditions. J Biol Chem 276, 43407–43412.

Pedersen PL (2007). The cancer cell's "power plants" as promising therapeutic targets: an overview. J Bioenerg Biomembr 39, 1–12.

Peschiaroli A, Giacobbe A, Formosa A, Markert EK, Bongiorno-Borbone L, Levine AJ, Candi E, D'Alessandro A, Zolla L, Finazzi Agrò A, *et al.* (2013). MiR-143 regulates hexokinase 2 expression in cancer cells. Oncogene 32, 797–802.

Qin Y, Cheng C, Lu H (2016). MiR-4458 suppresses glycolysis and lactate production by direct targeting hexokinase2 in colon cancer cells. Biochem Biophys Res Commun 469, 37–43.

Rempel A, Mathupala SP, Pedersen PL (1996). Glucose catabolism in cancer cells: regulation of the Type II hexokinase promoter by glucose and cyclic AMP. FEBS Letters 385, 233–237.

Riddle SR, Ahmad A, Ahmad S, Deeb SS, Malkki M, Schneider BK, Allen CB, White CW (2000). Hypoxia induces hexokinase II gene expression in human lung cell line A549. Am J Physiol Lung Cell Mol Physiol 278, L407–L416.
Rose IA, Warms JV (1967). Mitochondrial hexokinase. Release, rebinding, and location. J Biol Chem 242, 1635–1645.
Semenza GL (2003). Targeting HIF-1 for cancer therapy. Nat Rev Cancer 3, 721–732.
Semenza GL, Roth PH, Fang HM, Wang GL (1994). Transcriptional regulation of genes encoding glycolytic enzymes by hypoxia-inducible factor 1. J Biol Chem 269, 23757–23763.
Shaw G, Kamen RA (1986). Conserved AU sequence from the 3′ untranslated region of GM-CSF mRNA mediates selective mRNA degradation. Cell 46, 659–667.
Shyu AB, Wilkinson MF (2000). The double lives of shuttling mRNA binding proteins. Cell 102, 135–138.
Simonnet H, Alazard N, Pfeiffer K, Gallou C, Béroud C, Demont J, Bouvier R, Schägger H, Godinot C (2002). Low mitochondrial respiratory chain content correlates with tumor aggressiveness in renal cell carcinoma. Carcinogenesis 23, 759–768.
Vo MT, Choi SH, Lee JH, Hong CH, Kim JS, Lee UH, Chung HM, Lee BJ, Park JW, Cho WJ (2017). Tristetraprolin inhibits mitochondrial function through suppression of α-Synuclein expression in cancer cells. Oncotarget 8, 41903–41920.
Warburg O (1956). On the origin of cancer cells. Science 123, 309–314.
Wilson JE (1995). Hexokinases. Rev Physiol Biochem Pharmacol 126, 65–198.
Wilson JE (2003). Isozymes of mammalian hexokinase: structure, subcellular localization and metabolic function. J Exp Biol 206, 2049–2057.
Woldetsadik AD, Vogel MC, Rabeh WM, Magzoub M (2017). Hexokinase II–derived cell-penetrating peptide targets mitochondria and triggers apoptosis in cancer cells. FASEB J 31, 2168–2184.
Wu M, Neilson A, Swift AL, Moran R, Tamagnine J, Parslow D, Armistead S, Lemire K, Orrell J, Teich J, *et al*. (2007). Multiparameter metabolic analysis reveals a close link between attenuated mitochondrial bioenergetic function and enhanced glycolysis dependency in human tumor cells. Am J Physiol Cell Physiol 292, C125–C136.
Yoon NA, Jo HG, Lee UH, Park JH, Yoon JE, Ryu J, Kang SS, Min YJ, Ju SA, Seo EH (2016). Tristetraprolin suppresses the EMT through the down-regulation of Twist1 and Snail1 in cancer cells. Oncotarget 7, 8931–8943.
Young LE, Sanduja S, Bemis-Standoli K, Pena EA, Price RL, Dixon DA (2009). The mRNA binding proteins HuR and tristetraprolin regulate cyclooxygenase 2 expression during colon carcinogenesis. Gastroenterology 136, 1669–1679.
Yu P, Wilhelm K, Dubrac A, Tung JK, Alves TC, Fang JS, Xie Y, Zhu J, Chen Z, De Smet F, *et al*. (2017). FGF-dependent metabolic control of vascular development. Nature 545, 224–228.